E3S Web of Conferences **371**, 03047 (2023) https://doi.org/10.1051/e3sconf/202337103047
AFE-2022

Longitudinal and transverse oscillations of the impact device tool under impulsive loads

Alexander Slidenko[1*] , *Viktor* Slidenko[2]

[1]JSC «Scientific Research Institute of Blade Machines», 394062 Voronezh, Russia
[2] National Technical University of Ukraine "Igor Sikorsky Kyiv Politechnic Institute", 03134 Kyiv, Ukraine

Abstract. The destruction process of the rock by the tool of the impact device occurs with an impulsive load on the tool from the recoil reaction from the side of the rock, not only in the axial, but also in the transverse direction. A model of the tool part of the impact device is considered, which takes into account the transverse and longitudinal tool oscillations. The tool model has the form of a rod for longitudinal loading and a beam of constant cross section for transverse loading. Transverse and longitudinal oscillations of the tool sections are considered independent. When calculating transverse oscillations, the tool is considered as a cantilever beam with a rigid mount at one end. The calculation scheme of longitudinal oscillations is represented by a rod with reduced elastic resistance at the end. Impulsive loads are modeled by the initial velocity distribution on the contact part of the tool. The initial-boundary value problem with wave equations of the second and fourth orders is formulated. The solution of the initial-boundary value problem by the Fourier method, realized in the Mathcad system, is proposed.

1 Introduction

The study of the interaction of the impact device tool with the working environment was carried out by a number of authors [1-7]. In the works, longitudinal oscillations arising under the action of axial impulsive loads were considered. Loads from the side of the striker [3-8] and also, as a recoil reaction, from the side of the processed rock [9,10] were considered. Impulsive loads were modeled by the initial velocity distribution along the length of the tool [11]. It should be noted that when the tool interacts with the processed medium, transverse impulsive loads occur, which lead to transverse oscillations of the tool. In the works [12, 13] the studies of transverse oscillations of a constant cross section beam were carried out under various transverse loads and ways of fastening the beam. The formulated initial boundary value problems were solved by the Fourier method. The study of transverse and longitudinal oscillations of the impact device tool allows to get a more complete picture of the stresses that occur in the cross sections of the tool.
The purpose of the work is to build a model that takes into account the asymmetric impulsive load, as a recoil reaction from the rock, on the working end of the tool. It is aimed to solve the formulated initial-boundary value problems by the Fourier method and present the results in a common computer program.

* Corresponding author: alexandr.slidenko@yandex.ru

 https://doi.org/10.1051/e3sconf/202337103047

The following tasks are solved in the research process:
1) An initial-boundary value problem is formulated for the transverse and longitudinal oscillations of a tool with a round cross section with a rigid fastening in the transverse direction and taking into account the elastic resistance in the longitudinal direction;
2) The initial boundary value problem is solved by the Fourier method;
3) The decision analysis is carried out using the program in the Mathcad system.

2 Setting of the initial-boundary value problem

The diagram of the load on the tool of the impact device by the recoil reaction from the side of the processed rock is shown in Fig.1.

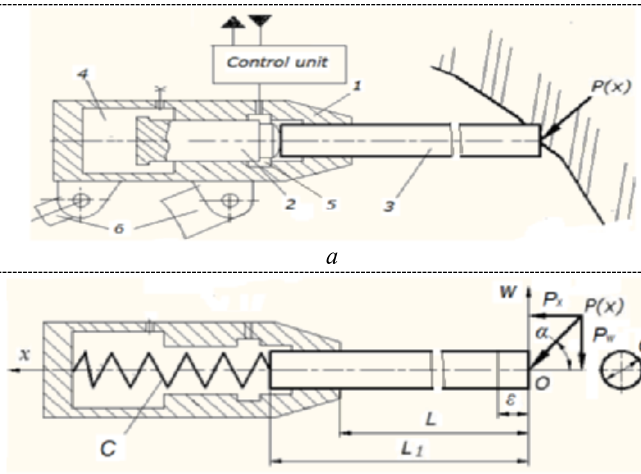

Fig. 1. The diagram of the load on the tool of the impact device mounted on the manipulator: *a*) structural diagram of the impact device: 1 – body of the impact device, 2 – a striker, 3 – a tool, 4 – pneumatic accumulator chamber, 5 – control chamber, 6 –structural elements of the manipulator, *P(x)* – recoil reaction; *b*) the design scheme of the tool load: *Px, Pw*– the components of the recoil reaction, *C* – unit stiffness of the impact device elements (striker and pneumatic accumulator); ε , *L*, L_1– dimensions of the edge section, the cantilever part and the tool as a whole, *d*– tool diameter, *x*–coordinate axis.

The structural diagram (Fig. 1, *a*) of the impact device, mounted on the manipulator, includes a striker 2 and a tool 3 coaxially located in the body 1. Moreover, the pneumatic accumulator 4 is charged by the mechanism for cocking the striker 2 with a working fluid, which is alternately supplied through the control chamber 5, which has an alternating hydraulic connection through the control device, with the hydraulic pressure and drain lines, respectively. At the same time, the striker moves and compresses the working medium, for example, neutral gas is carried out its energy charging in the chamber of the pneumatic accumulator when it is connected to the pressure line of the control chamber. When the control chamber is connected to the drain line, the pneumatic accumulator is discharged and, in its final phase, the striker strikes the tool. Taking into account the different position of the tool relative to the processed medium, the direction of the recoil reaction at a certain angle to the tool axis is the most likely case. Based on the structural scheme (Fig. 1, a), a design scheme (Fig.1, b) is given, which includes a tool with a constant circular cross section, loaded with the initial recoil reaction impulse or the distribution of the initial displacement. It is supposed to limit the movement of the tool as a rigidly fixed beam at one end in the transverse direction and elastic resistance to the movement of the tool in the longitudinal direction.

The transverse oscillations of the tool, like beams of constant section, are described by fourth-order differential equations (1), and the longitudinal oscillations of the tool are described by second-order equations with partial derivatives (2):

$$\frac{\partial^4 w(t,x)}{\partial x^4} + a^4 \frac{\partial^2 w(t,x)}{\partial t^2} = 0, \quad x \in (0,L), \quad t \in (0,\theta) \tag{1}$$

$$\frac{\partial^2 u(t,x)}{\partial t^2} = a_x^2 \frac{\partial^2 u(t,x)}{\partial x^2} \quad x \in (0,L_1) \tag{2}$$

where E–the modulus of elasticity of the tool material, J – the moment of inertia of the cross section, $J = \pi d^4 / 64$, ρ – the density of the tool material, S –the cross section area, $S = 0.25\pi d^2$, $a_x = \sqrt{E \cdot \rho^{-1}}$, $a^4 = \rho S (EJ)^{-1}$, $w(t,x)$– the transverse displacement of the tool x section at time t, $u(t,x)$ – the longitudinal displacement of the section x of the rod. Assumed the shape of beam fastening determines the type of boundary conditions. With a cantilever rigid limitation of transverse displacements, the boundary conditions have the form

$$w(t,L) = 0, \quad \frac{\partial w(t,L)}{\partial x} = 0 \tag{3}$$

$$\frac{\partial^2 w(t,0)}{\partial x^2} = 0, \quad \frac{\partial^3 w(t,0)}{\partial x^3} = 0, \quad t \in (0,\theta) \tag{4}$$

For longitudinal displacements, the boundary conditions have the form

$$ES \frac{\partial u}{\partial x}(t, L_1) = -C \cdot u(t, L_1), \quad ES \frac{\partial u}{\partial x}(t,0) = 0 \tag{5}$$

Initial conditions:

$$u(0,x) = f_1(x), \quad \frac{\partial u}{\partial t}(0,x) = F_1(x), \quad x \in [0, L_1] \tag{6}$$

$$w(0,x) = f_2(x), \quad \frac{\partial w}{\partial t}(0,x) = F_2(x), \quad x \in [0, L] \tag{7}$$

$$F_1(x) = \begin{cases} \dfrac{P_x}{\rho S \varepsilon}, if \ \ 0 \le x \le \varepsilon, \\ 0, \quad if \quad \varepsilon < x \le L_1. \end{cases} \tag{8}$$

$$F_2(x) = \begin{cases} \dfrac{P_w}{\rho S \varepsilon}, if \ \ 0 \le x \le \varepsilon, \\ 0, \quad if \quad \varepsilon < x \le L. \end{cases} \tag{9}$$

where $P_x = P(x)\cos\alpha$, $P_w = P(x)\sin\alpha$. Conditions (3) mean the absence of displacement and rotation in the section $x = L$. Conditions (4) express the fact that there is no resistance to transverse displacement and bending in the section $x=0$. The functions $f_1(x)$ and $f_2(x)$ set the initial distribution of the longitudinal and transverse displacements of the tool sections along the length $f(x)$, the functions $F_1(x)$ $F(x)$ and $F_2(x)$ set the distribution of the longitudinal and transverse velocities of the tool sections along its length at the initial moment of time. The shock impulse is modeled by the distribution of the initial velocity in a finite small section ε (Fig. 1) [9–11]. The parameter ε is chosen based on the results of computational experiments in the range $(0.1...0.2)L$ for longitudinal and transverse impulse loads.

3 The solution of the initial-boundary value problem by the Fourier method

The solution of the problem can be found by the method of separation of variables [13 - 15]. Let us consider this method for the longitudinal and transverse displacements of the tool sections. The solution of equation (2) has the form of a product of two functions

$$u(t,x)=T(t)\cdot X(x) \tag{10}$$

The boundary eigenvalue problem for a function $X(x)$ has the form:

$$X''+\lambda^2 X=0\ ,\quad X'(0)=0\ ,\quad ES\cdot X'(L_1)=-C\cdot X(L_1) \tag{11}$$

General solution of differential equation (11):

$$X(x)=C_1\cos\lambda x+C_2\sin\lambda x$$

From the first boundary condition (11) we get

$$X(x)=\cos\lambda x \tag{12}$$

From the second boundary condition, we find the values l, by solving numerically in the Mathcad system using the *root*(…) function of the equation

$$\frac{ES}{L_1 C}\mu=ctg\mu \tag{13}$$

where $\mu=\lambda L_1$. Diagrams of the left and right parts of equation (13) and the Mathcad program with an error estimation are shown in Fig. 2.
The general solution of the second equation (14), relatively to the function $T(t)$

$$T''(t)+a_x^2\lambda^2 T(t)=0 \tag{14}$$

has the form

$$T(t)=A\cos(a_x\lambda t)+B\sin(a_x\lambda t) \tag{15}$$

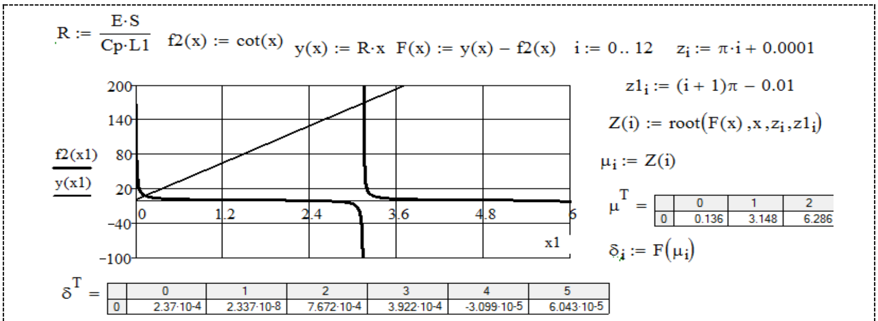

Fig. 2. The solution of equation (13) in the *Mathcad system using root(...)function: C = 5.6 10^6 N/m; a=5189 m/s.*

The dynamic parameters of a hydraulic hammer with an impact energy of 3...5 kJ, for example, a hydraulic hammer GPM-300, were taken for the study.
Particular solutions of the oscillation equation that satisfy the boundary conditions are obtained for various values $\lambda_k = \dfrac{\mu_k}{L}$, $k = 1,2,...$ Let us make a functional series

$$u(t,x) = \sum_{k=1}^{\infty} \left(A_k \cos(a_x \lambda_k t) + B_k \sin(a_x \lambda_k t)\right) \cos \lambda_k x \tag{16}$$

The constants A_k and B_k are chosen so that the initial conditions (6) are satisfied

$$u(0,x) = \sum_{k=1}^{\infty} A_k \cos \lambda_k x = f_1(x), \quad \frac{\partial u(0,x)}{\partial t} = \sum_{k=1}^{\infty} a_x \lambda_k B_k \cos \lambda_k x = F_1(x) \tag{17}$$

As a result of the transformations, formulas for determining the coefficients of the Fourier series were obtained:

$$A_k = \frac{4\mu_k}{L(2\mu_k + \sin 2\mu_k)} \int_0^L f_1(x) \cos \frac{\mu_k}{L_1} x dx, \quad B_k = \frac{4}{a_x(2\mu_k + \sin 2\mu_k)} \int_0^L F_1(x) \cos \frac{\mu_k}{L_1} x dx.$$

The coefficients B_k where $\varepsilon \to 0$ have limiting values, i.e.

$$B_k = \frac{4P_x}{a_x(2\mu_k + \sin 2\mu_k) S\rho} \tag{18}$$

Fig. 3, *a* shows the solution over a long time interval, Fig. 3,*b* shows the solution on a small interval. The exclusion of the first term of the Fourier series made it possible to separate the deformation of the rod from the displacement due to the deformation of the elastic element. The first term of the Fourier series reflects the motion of the rod as a discrete element, the mass of which is equal to the mass of the rod, for a given incentive impulse. This can be shown by comparing the solution (20) of the initial problem (19) with the first term of the Fourier method (Fig. 4).

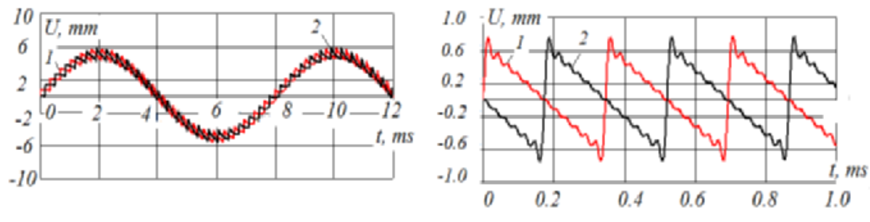

Fig. 3. Longitudinal oscillations of the rod: *1) U(t,0), 2) U(t,L₁), Px=394 Ns; α=10⁰, d=0,135m; L=1m, ε=0,2m, 1) U(t,0), 2) U(t,L)*; *a*) the first 12 members of the series; *b*) the first member of the series is missing.

$$m\frac{d^2y(t)}{dt^2}=-C\cdot y(t),\quad y(0)=0,\quad \frac{dy(0)}{dt}=V_0 \tag{19}$$

$$y(t)=\sqrt{\frac{m}{C}}\cdot V_0\cdot\sin\left(\sqrt{\frac{C}{m}}\cdot t\right). \tag{20}$$

Moreover, the initial speed is determined from the condition of equality of the initial impulses applied to the rod and to the discrete mass:

$$V_0=\frac{P_x}{m}=\frac{P_x}{\rho SL_1}.$$

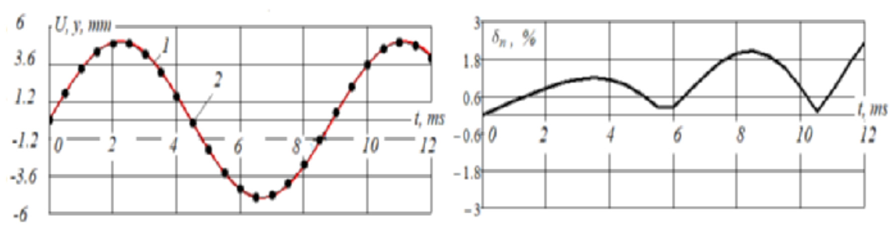

Fig. 4. *a*) Comparison of solutions: 1) the first term of the series; 2) solution (20) of the initial problem *b*) relative difference of solutions.

The relative difference between the solutions was less than 3% (Fig. 4, *b*).
Let us consider the method of separation of variables for equation (1), which is similar to the method for equation (2). The solution must be looked for in the form of a product of two functions, one of which depends only on *x*, the other function depends only on *t*. So the solution should have the form

$$w(t,x)=U(x)\cdot V(t). \tag{21}$$

After substituting the derivatives into equation (1), we have the equality

$$V(t)\frac{d^4U(x)}{dx^4}=-a^4U(x)\frac{d^2V(t)}{dt^2}. \tag{22}$$

After separating the variables, we obtain an identical equation from which it follows that the represented ratio is a constant

$$\frac{1}{U}\frac{d^4U}{dx^4}=-a^4\frac{1}{V}\frac{d^2V}{dt^2}=+\lambda^4. \tag{23}$$

We obtain two ordinary differential equations of the fourth and second orders with constant coefficients with this choice of constant ($+\lambda^4$):

$$\frac{d^4U(x)}{dx^4}-\lambda^4U(x)=0, \tag{24}$$

$$\frac{d^2V(t)}{dt^2}+\left(\frac{\lambda}{a}\right)^4V(t)=0. \tag{25}$$

Solving the boundary value problem for eigenvalues, we first find the general solution of the fourth-order differential equation (24). The differential equation corresponds to the characteristic equation

$$k^4-\lambda^4=0. \tag{26}$$

This equation has four roots: two real and two complex:

$$k_{1,2}=\pm\lambda;\quad k_{3,4}=\pm i\lambda.$$

The general solution of equation (25) is taken in the form

$$U(x)=C_1\sin\lambda x+C_2\cos\lambda x+C_3 sh\lambda x+C_4 ch\lambda x \tag{27}$$

In solution (28), C_1, C_2, C_3, C_4 are arbitrary constants. To determine the constants C_1, C_2, C_3 and C_4, we use the boundary conditions (3) and (4).
We get equations

$$T(t)\cdot U(L)=0\Rightarrow U(L)=0,\quad V(t)\frac{dU(L)}{dx}=0\Rightarrow\frac{dU(L)}{dx}=0$$

$$T(t)\cdot \mathcal{U}(0)=T(t)\mathcal{U}(L)=0\Rightarrow \mathcal{U}(0)=\mathcal{U}(L)=0. \tag{28}$$

Performing transformations in a similar way, we obtain the boundary conditions for *U(x)* at $x=0$:

$$\frac{d^2U}{dx^2}(0)=\frac{d^3U}{dx^3}(0)=0. \tag{29}$$

We write down the system of equations for determining the constants using the boundary conditions (28) and (29):

$$\begin{cases} C_1\sin\lambda L+C_2\cos\lambda L+C_3 sh\lambda L+C_4 ch\lambda L=0,\\ C_1\cos\lambda L-C_2\sin\lambda L+C_3 ch\lambda L+C_4 sh\lambda L=0,\\ -C_2+C_4=0,\\ -C_1+C_3=0; \end{cases} \tag{30}$$

The system of equations (30) is homogeneous and has nonzero solutions when the determinant is equal to zero, or

$$\cos\lambda L\cdot ch\lambda L+1=0. \tag{31}$$

 https://doi.org/10.1051/e3sconf/202337103047

We introduce a function $\Phi(x) = \cos x + \frac{1}{chx}$ and we find a solution to the equation by the method of successive approximations

$$\Phi(x) = \cos x + \frac{1}{chx} = 0 \quad (32)$$

The diagram of the function and a program fragment of searching for an approximate solution of equation (32) in the Mathcad system are shown in fig. 5.

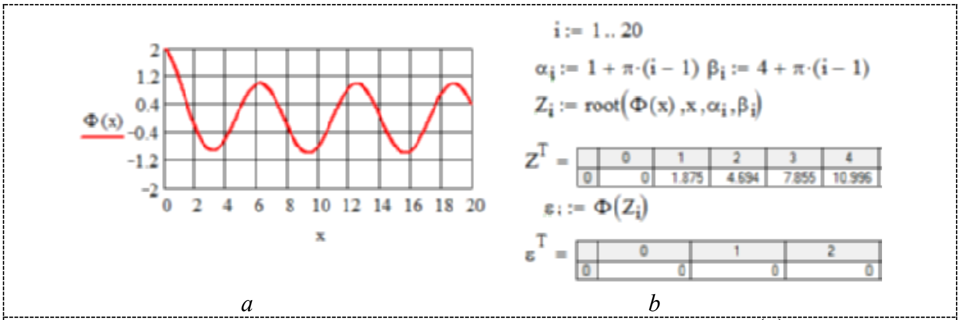

Fig. 5. *a*) The diagram of the function Φ(x); *b*) solution of the equation $\Phi(x) = 0$.

We get the formula for the eigenvalues of the boundary value problem and the eigenfunctions:

$$\lambda L = Z_n, n = 1,2,... \quad \lambda = \lambda_n = \frac{Z_n}{L} \quad (33)$$

$$U_n(x) = C_1(\sin \lambda_n x + sh\lambda_n x) + C_2(n)(\cos \lambda_n x + ch\lambda_n x) \quad (34)$$

From the system (30) at $C_1=1$ we get

$$C_2(n) = -\frac{\sin \lambda_n L + sh\lambda_n L}{\cos \lambda_n L + ch\lambda_n L}.$$

Thus, the eigenfunctions of the boundary value problem have the form

$$U_n(x) = (\sin \lambda_n x + sh\lambda_n x) - \left(\frac{\sin \lambda_n L + sh\lambda_n L}{\cos \lambda_n L + ch\lambda_n L}\right)(\cos \lambda_n x + ch\lambda_n x) \quad (35)$$

The characteristic equation for differential equation (25) is written as

$$k^2 + \left(\frac{\lambda}{a}\right)^4 = 0 \quad (36)$$

The equation (37) has complex conjugate roots (purely imaginary):

$$k_{1,2} = \pm\left(\frac{\lambda}{a}\right)^2 i \quad (37)$$

The general solution of differential equation (25) has the form

 https://doi.org/10.1051/e3sconf/202337103047

$$V(t) = C_1 \cos\left(\frac{\lambda}{a}\right)^2 t + C_2 \sin\left(\frac{\lambda}{a}\right)^2 t \tag{38}$$

In equation (38), C_1 and C_2 are arbitrary constants. For each value $\lambda = \lambda_n$ we have linearly independent solutions. Independent solutions of equation (1) satisfy the boundary condition and will have the form:

$$w_n(t,x) = T_n(t)\cdot U_n(x) = \left(A_n \cos\left(\frac{\lambda_n}{a}\right)^2 t + B_n \sin\left(\frac{\lambda_n}{a}\right)^2 t \right)\cdot U_n(x) \,. \tag{39}$$

To perform the initial conditions (4), a series is made

$$w(t,x) = \sum_{n=1}^{\infty} w_n(t,x) = \sum_{n=1}^{\infty} \left(A_n \cos\left(\frac{\lambda_n}{a}\right)^2 t + B_n \sin\left(\frac{\lambda_n}{a}\right)^2 t \right) U_n(x) \,. \tag{40}$$

From the initial condition (4) it follows

$$w(0,x) = \sum_{n=1}^{\infty} A_n U_n(x) = f_2(x) \,. \tag{41}$$

Multiplying both sides of identity (41) by $U_n(x)$ and integrating, we obtain

$$\int_0^L f_2(x)\cdot U_n(x)dx = \int_0^L A_n U_n^2(x)dx \,.$$

From here we obtain a formula for calculating the coefficients of the Fourier series

$$A_n = \left(\int_0^L U_n^2(x)dx \right)^{-1} \cdot \int_0^L f_2(x) U_n(x)dx \,. \tag{42}$$

We get the formula for calculating the coefficient B_n :

$$B_n = a^2 \left((\lambda_n)^2 \cdot \int_0^L U_n^2(x)dx \right)^{-1} \int_0^L F_2(x) U_n(x)dx \,. \tag{43}$$

4 The interval calculation of the Fourier series in the Mathcad system

The initial velocity distribution along the length of the tool is shown in fig. 6, a. The initial impulse load is applied to the right free part of the tool. The velocity distribution of the cross sections of the beam according to formula (9) simulates an external transverse impact. It is also possible to set the initial distribution of transverse displacements along the length of the shaft (Fig. 6, b).

 https://doi.org/10.1051/e3sconf/202337103047

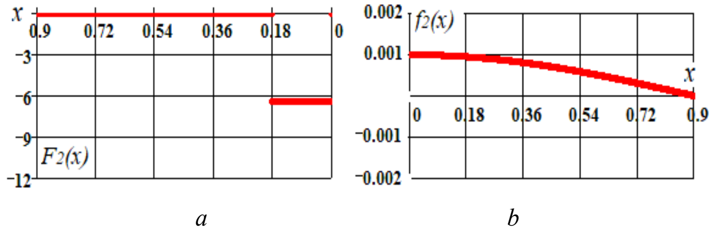

Fig. 6. *a)* Initial velocity distribution of beam cross sections;
b) Initial distribution of displacements of beam cross sections.

The distribution of transverse displacements and velocities is shown in Fig.7. Fourier series coefficients are calculated in the Mathcad system. The transverse displacement of the shaft sections is calculated in the presence of the first ten terms of the Fourier series.

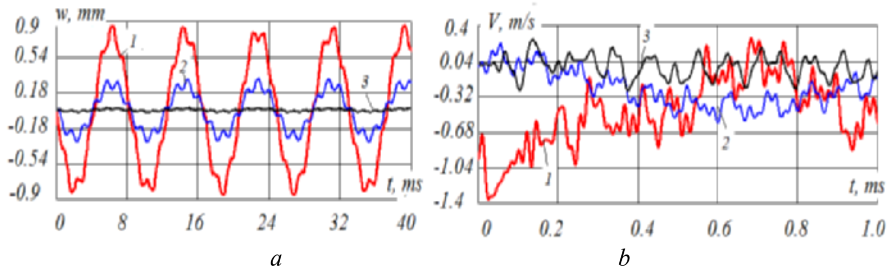

Fig. 7. *a*) Displacements of various beam sections in time in the presence of only the initial impulse load: *b*) Dependence of speed on time for various sections of the tool: *L=0.9 m*; *d=0.135m; P_w=17.45 Ns; 1) x = L/2 m; 2) x =3L/4 m; 3) x =9L/10 m.*

The deflection beam shape at a given time is shown in Fig. 8,*a* in the presence of a finite number of terms in the Fourier series.

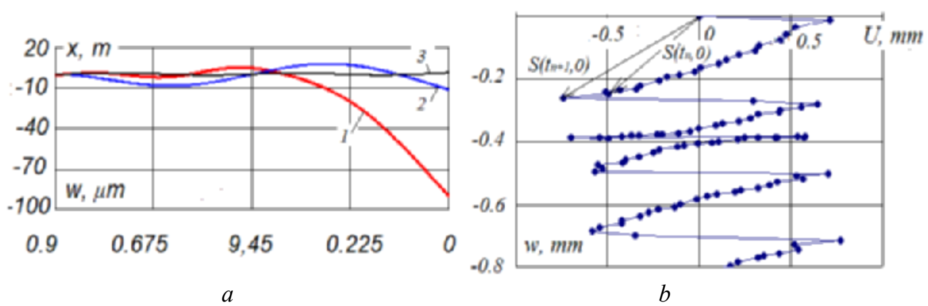

Fig. 8. *a*) Transverse beam deflection at t = *80 µs:* (1) 10 terms of the series; (2) the third term of the series; (3) the fifth term of the series; *b*) The total deformation of the section *x=0* in the plane *Oxw* time period [0, 3.3] *ms.*

The total displacement of the tool in time is of interest. The displacement area can be obtained by excluding time, that means, to plot in the phase plane O*xw* and determine the vector sum of the transverse and longitudinal $S(t_n, x_i)$ (Fig. 8,*b*).
The obtained diagrams for various sections of the tool give an idea of the change area of the longitudinal and transverse displacements of the cross sections of the tool.

5 Conclusion

As a result of this work we can conclude as follow.
1. A mathematical model is proposed that takes into account the asymmetric load on the tool face of the impact device from the side of the processed rock. The model assumes an independent division of the load into axial and transverse components. The shock impulse is modeled by the distribution of the initial velocity over a short length of the contact part of the tool. The equations for transverse and longitudinal oscillations are separated for different initial and boundary conditions.
2. The solution of the initial-boundary value problem with wave equations for longitudinal and transverse oscillations under an impulse initial load is found by the Fourier method using the built-in functions of the Mathcad system in a common computer program. The program allows you to highlight the main forms of oscillations in the transverse and longitudinal directions.
3. The analysis of solutions obtained by the Fourier method in the Mathcad system was carried out. The amplitudes of the transverse and longitudinal displacements of the tool sections, the total displacement of the tool sections, built in the phase plane with the exception of time, are estimated. When changing the angle of inclination of the tool within (0-10^0) at a pulse of *(300 -500) Ns*, the ranges of parameters of transverse and longitudinal oscillations of the contact part of the tool were obtained. It must be taken into account when designing impact devices to ensure the required reliability.

References

1. A.P. Ivanov, System Dynamics with Mechanical Collisions (Moscow, International Education Program, 1997)

2. V.K. Manzhosov, V.V. Slepukhin, The Modeling of Longitudinal Impactin Frameworksofa Heterogenious Structure (Ulyanovsk, Ul. STU, 2011).

3. A.D. Batako, V.I. Babitsky, N. A. Halliwell, Journal of sound and Vibration, **V 271** (2004)

4. V.K. Manzhosov, Longitudinal impact Models (Ulyanovsk, Ul STU, 2006)

5. V.K. Manzhosov, D.A. Novikov, Modeling of transient and limit motion cycles of vibro-shock systems with discontinuous characteristics (Ulyanovsk, Ul STU, 2015)

6. I.A. Zhukov, V.V. Molchanov, Advanced Materials Research, **V 1040** (2014)

7. I.A. Zhukov, L.T. Dvornikov, S.M. Nikitenko, IOP Conference Series: Materials Science and Engineering **V 1241,** 012171 (2016)

8. I.A. Zhukov, A.A. Repin, E.G. Timofeev, IOP Conf. Series: Earth and Environmental Science **134** 012071 (2018) https://doi.org/10.1088/1755-1315/134/1/012071

9. A.M. Slidenko, V.M. Slidenko, Journal of Physics: Conference Series **1203,** 012086 (2019) https://doi.org/10.1088/1742-6596/1203/1/012086

10. V.M. Slidenko, A.M. Slidenko, Mathematical Modeling of Shok-wave Processes of Hydropulse System of Mining Machines (Kyiv, KPI alter Igor Sikorski, Polytechnic, 2017)

11. I.G. Aramanovich, V.I Levin, Equations of Mathematikal Physics (Moscow, Science, 1969)

12. V.S. Doev, Transverse oscillations of the beams (Moscow, KNORUS, 2016).

13. T.Y. Nikitina, Herald of the State University of Sea and River Fleet named after Admiral S. O. Makarov **3(22)** (2013)

14. M.S. Koshlyakov, E.B. Gliner, M.G. Smirnov, Equations in Partial Derivatives of Mathematikal Physics (Moscow, Higher School, 1970)
15. A.M. Slidenko, V.M. Slidenko, Journal of Physics: Conference Series **1902,** 012024 (2021) https://doi.org/10.1088/1742-6596/1902/1/012024